898 (1969). These authors discuss the analogy between their magnetic problem and the superfluid situation. They argue that if Ψ and n_0 are not equal, then additional terms $b_k(\delta\Psi - \delta n_0)$ should in principle be included in the hydrodynamic equations (for example, in the $\dot{v}_s$ equation). The coefficients of such terms vanish by symmetry considerations in the planar ferromagnet, but are not automatically zero in the superfluid. Their discussion involves a frequency-independent relaxation time τ_k for Ψ, and they illustrate various possibilities for τ_k and the coefficients like b_k which will guarantee that two-fluid hydrodynamics is valid, in particular, that the usual analysis of second sound applies. They suggest that the most likely possibility is that τ_k may diverge as $k \to 0$, but that the coefficients like b_k go to zero sufficiently rapidly so that the familiar two-fluid model predictions concerning the damping rate of second sound remain valid. The divergence of τ_k as $k \to 0$ can destroy dynamic local equilibrium for Ψ, but nothing is changed in the second sound analysis. In terms of our discussion, we have set the coefficients $b_k = 0$ from the start (or $b_k \to 0$ so rapidly with k that such coefficients remain outside the hydrodynamic low k discussion), since we have used Eqs. (5) throughout. As we have shown, one can describe our results with an analogous $\tau_k(\omega + i\delta)$. This function depends on both k and ω, but it diverges in the critical limit

$$\lim_{k \to 0} \mathrm{Re}\tau_k(\omega + i\delta) = \pi\left(\frac{n_0}{n}\right) n \frac{\partial}{\partial n}\frac{n_0}{n}\Big|_s \delta(\omega).$$

Although the behavior of our $\tau_k(\omega + i\delta)$ is somewhat more complicated, one can trace our lack of dynamic local equilibrium to this critical limit. The actual condition for dynamic local equilibrium is of course $\omega\tau_{\omega/u}(\omega + i\delta) \ll 1$ for hydrodynamic frequencies, and this is not satisfied in our case. Our conclusions are thus in agreement with one of the possibilities discussed by Halperin and Hohenberg. The difference is that our τ is fully determined by the hydrodynamic parameters. There is also a conceptual difference in approach, since we begin with a conservation-law structure for Ψ. The discussion in terms of a relaxation time $\tau_k(\omega + i\delta)$ is not a natural one for our analysis.

PHYSICAL REVIEW A VOLUME 2, NUMBER 4 OCTOBER 1970

Superfluid Critical-Velocity Measurements Utilizing Phase Coupling*

H. E. Corke† and A. F. Hildebrandt
Department of Physics, University of Houston, Houston, Texas 77004
(Received 2 April 1970)

Quantum-mechanical phase coherence in He II produces a coupling between elements of the superfluid that places restrictions upon the flow. This phase coupling was utilized in the flow of superfluid through wide ($> 10^{-3}$ cm) parallel channels to detect the first sign of flow impedance. A sensitive pressure-measuring device located in one of the channels was used to monitor the velocity and detect the superfluid critical velocity. Isothermal, as well as heat current flow, was investigated in the temperature range 1.71–2.15 °K. The results substantiate the presence of phase coupling and indicate that a superfluid critical velocity exists, which agrees with the concept of vortex generation and is not influenced by normal fluid flow. Channel-size dependence was found to be approximately d^{-1} with only a small temperature dependence. At velocities well above critical, flow transitions were observed which indicated the onset of superfluid turbulence. The values of these turbulent critical velocities compare favorably with past data which give a channel-size dependence of $d^{-1/4}$.

INTRODUCTION

Critical-velocity measurements in wide channels using pure superfluid or isothermal flow have been made recently by van Alphen *et al.*[1] Their data indicate that v_{sc} varies with channel size as $d^{-1/4}$ like narrow-channel critical velocities. These values for wide channels agree with the work of Chase[2] in flow near the λ point, that of Craig and Pellam[3] in a superfluid wind tunnel, and that of Kramers[4] using second-sound attenuation. However, most of the older critical-velocity data are much lower in value and are more closely dependent upon channel size as d^{-1}. Van Alphen suggests that the lower reported critical velocities are the result of observing classical normal-fluid turbulence. At low temperature, experiments with high normal-fluid velocities are realized in heat currents where only a small percentage of the hel-

ium is normal fluid. Other critical-velocity experiments not involving heat currents but with the possibility of normal-fluid interference are U-tube oscillations,[5] and rotating disks and cylinders.[6] All of these experiments report critical velocities in the lower range.

There is evidence, however, that dissipation in the form of vortices is generated for superfluid flow in wide channels at lower reported critical velocities. For example, Trela and Fairbank[7] have measured the energy loss of superfluid flow through orifices by U-tube oscillations. They found that lossless flow occurs below a critical velocity which agrees with the Onsager-Feynman vortex model.[8,9] Another experiment, using isothermal superfluid flow in wide channels, was performed by Chung.[10] He observed that a mixture of suspended hydrogen and deuterium gases produced three characteristic flow regions. At low velocities, the particles remained stationary, indicating potential flow. Above a certain velocity, motion with the flow was observed, indicating the creation of vortices and drag. At a higher velocity, large random motion set in, indicating turbulent flow. A similiar effect was also observed for heat currents in wide channels.[11]

Recently, quantum effects in He II have best been explained by ascribing to the superfluid a long-range phase coherence. This couples elements of the superfluid in such a manner that the flow profile has certain restrictions. Ultilizing the idea of phase coupling, Hammel[12] has outlined a method to generate persistent currents in doubly connected superfluid helium. Referring to Fig. 1, when superfluid is pumped from left to right the amount of flow through each channel is governed by the phase coupling. Consider, for simplicity, that there is zero circulation,

$$\int \vec{v}_s \cdot d\vec{l} = nh/m = 0 \ , \qquad (1)$$

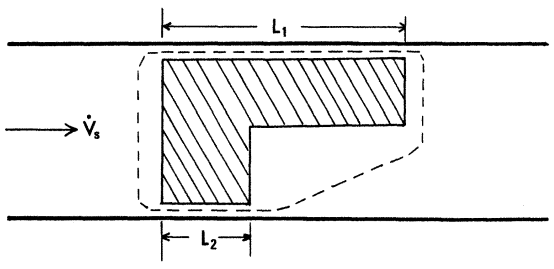

FIG. 1. Doubly connected region formed by two parallel channels C-I and C-II of length L_1 and L_2. $\dot{V}_s$ is the superfluid volume flow rate, the dashed line is the path of the circulation integral.

around the dashed line. With the channel cross-sectional areas equal and much smaller than other parts of the system, the contributions to the line integral are mainly along the channels. Then, with the identity

$$\vec{v}_s = (h/m)\,\nabla\phi \ , \qquad (2)$$

where ϕ is the phase of the wave function, and disregarding the small velocities outside the channels, the phase shift through each channel is the same; that is, $\Delta\phi = v_{s1}L_1 = v_{s2}L_2$. This indicates that the velocity v_{s2} in the shorter channel is larger than v_{s1} by L_1/L_2. Increasing the total volume flow rate $\dot{V}_s$ eventually causes v_{s2} to reach critical velocity first. Should v_{s2} exceed critical velocity, a pressure drop would normally develop across channel II, but this cannot happen because the flow through channel I is still potential. Therefore, v_{s2} remains constant at or just below the critical velocity as $\dot{V}_s$ is increased further. Channel I acquires all the additional flow increase until v_{s1} reaches critical velocity. After v_{s2} reaches critical velocity and remains constant there is phase slippage along channel I, and the circulation around the channels builds in units of h/m as v_{s1} increases to critical velocity. This circulation will continue to flow or persist when $\dot{V}_s$ is reduced to zero if the phase coupling is strong enough or not disrupted. However, if $\dot{V}_s$ is increased from the point where v_{s1} goes critical the flow will again increase in channel II, both channels being above critical velocity. Monitoring v_{s2} and knowing $\dot{V}_s$ as it is increased, the critical velocity in both channels can be determined.

Experimental support for the ideas just described has been reported by van Alphen[13] for flow in narrow channels. The persistent superfluid or "persistatron" was produced in a 46-cm-long circuit consisting of two parallel channels of different lengths, packed with jeweler's rouge. This macroscopic persistent flow was observed by measuring the kinetic energy released when the circulation was disrupted.

It is the intent of this research to demonstrate and utilize phase coupling for superfluid flow in parallel channels to detect the velocity where the first sign of flow impedance occurs. The critical superfluid velocity is observed directly by measuring the Bernoulli pressure change due to the flow. Isothermal flow and heat currents are investigated for wide channels over a temperature range of 1.71–2.15 °K. Therefore, dependence of critical velocities upon channel size, temperature, and the effect of heat currents is obtained.

APPARATUS

The experimental apparatus can be divided into two separate parts: a channel assembly with cal-

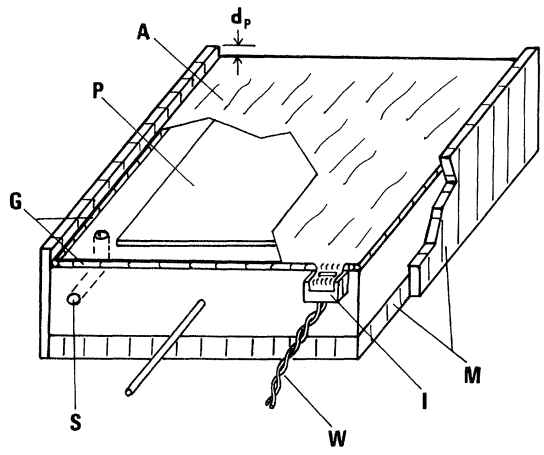

FIG. 2. Velocity Probe. A is a thin aluminum-foil membrane stretched and secured to glass fibers G; P is polished-aluminum plateau on the aluminum base; S is a static-pressure port; W is a twisted copper wire for the electrical ground connection; I is a phenolic insulating block; M denotes phenolic plates for electrical insulation; and d_p is the depth of the velocity-probe channel.

ibration section and a velocity-measuring system. Two different apparatuses were constructed and used in this experiment to measure critical velocity. From Bernoulli's equation, the pressure due to the steady-state flow of superfluid is equal to $\frac{1}{2}\rho_s v_s^2$. Below critical velocity this is the only pressure present as the result of the flow. To measure this pressure and determine the superfluid velocity, a pressure-sensing device was constructed in one wall of a channel through which the superfluid flowed. This section of the wall was a thin aluminum-foil membrane which functioned as one plate of a capacitor in a parallel L-C tuned back diode oscillator. Displacements of the foil due to pressure changes altered the value of the capacitor and changed the oscillator frequency. Therefore, superfluid velocity was detected as a frequency change.

Construction of the pressure-sensing device, referred to as a velocity probe in Fig. 2, started with an aluminum block 1 cm square and 0.358 cm thick. On top of the block, a polished plateau P was machined 0.75 cm square and 0.007 cm high. Four glass fibers B, approximately 0.01 cm diam, were epoxied in place around the top edge of the aluminum block. A metal spacer 0.8 cm square and 8.9×10^{-4} cm thick was placed on the plateau and the glass fibers were ground down to this spacer by using aluminum-oxide powder on a flat glass plate. The plateau was then about 10^{-3} cm below the ground surfaces of the glass fibers. A small phenolic block I with two parallel 0.025-cm holes was epoxied to the aluminum block as shown.

Aluminum-foil A approximately 10^{-4} cm thick was secured with epoxy across the glass fibers. When the foil was trimmed around the edges of the aluminum block, a tab was left which was secured to the phenolic block I by silver conductive paint. A U-shaped copper wire W was placed through the foil tab, through the holes in the phenolic block and twisted to ensure good electrical contact for the ground connection. A copper wire was pressed into a hole in the front of the aluminum block for electrical connection to the oscillator. Phenolic plates M were epoxied to the bottom and sides of the aluminum block for electrical insulation. The top of the phenolic sides were carefully sanded off to a distance d_p above the aluminum-foil surface.

The phenolic plates of the velocity probe were lightly coated with epoxy and slipped into a holder which formed a channel d_p cm deep. The channel dimensions of the two probes that were used to obtain critical velocity data are listed in Table I. Static port S allowed free flow of helium in and out of the space between the aluminum foil and the aluminum block over which the foil was stretched. Therefore, the fluid pressure existing at this port entrance was impressed at all points under the foil, and pressure gradiants across the probe channel due to viscous flow or superfluid accelerations were detected as well as Bernoulli pressure changes. The plane of the foil was placed vertical to eliminate the effect of gravity which with the foil horizontal would have exerted a force on the foil 10 times the force due to superfluid flow near critical velocity.

A *G-E BD*-6 back diode was used in the design of the parallel L-C tuned oscillator. A similar circuit has been used by Reppy.[14] The diode and high-Q coil were mounted with the channel apparatus in the liquid helium to increase gain and stability. A mercury cell for the oscillator and a preamplifier were located outside the helium Dewar and connected to the diode by a tubular

TABLE I. Channel dimensions (cm).

Channel	d	Width	Area	Length
A	4.0×10^{-3}	0.81	3.21×10^{-3}	1.5
B	5.1×10^{-3}	0.495	2.5×10^{-3}	1.0
C	7.7×10^{-3}	0.902	6.88×10^{-3}	1.5
D	1.2×10^{-2}	0.398	4.74×10^{-3}	1.0
E	3.8×10^{-2}	16 holes	1.81×10^{-2}	0.5
F	5.1×10^{-2}	0.505	2.55×10^{-3}	1.0
Valve guide	i.d. = 0.467	o.d. = 0.477	9×10^{-3}	1.5
Probe 1	7×10^{-3}	1.0	7×10^{-3}	1.0
Probe 2	6×10^{-3}	1.0	6×10^{-3}	1.0

stainless-steel coax line. A frequency counter displayed the oscillator frequency, which was on the order of 16 MHz. A digital-to-analog converter selected the two least significant digits of the frequency and displayed the analog voltage on the y axis on an x-y recorder. This gave a 100-Hz full-scale display.

Basically the channel assemblies in Fig. 3, consisted of two precision channels C-I and C-II, jewelers-rouge porous plugs R, and resistance heaters H-1 and H-2 for pumping the superfluid. Five different rectangular channels were constructed by separating the flat polished surfaces of two half-round brass pieces with shim stock spacers. Brass sleeves were fitted snugly around the channel pieces and solder was applied to hold and seal the assembly. One other channel was made with 16 round holes drilled in a brass rod. The holes were reamed to insure that the channels were as smooth as possible. All the entrance and exit corners of the channels were rounded with a radius of curvature greater than the channel depth d. This insured that the velocity of the superfluid at the corners did not exceed the velocity in the main portion of the channel. The effect of sharp corners in a similar potential problem has been discussed by Hildebrandt *et al.*[15] for superconducting shells. Table I lists the dimensions of the six channels A–F. These measured values are estimated to be accurate within 5%.

The porous plugs R were tightly packed jewelers rouge encased in relatively long thin-walled (1.5×10^{-2} cm) copper cylinders. This construction minimized the conduction of added heat energy along the rouge which prevented unwanted heat currents at the other end. The heat, instead, flowed radially outward through the thin-walled copper cylinder to the helium bath.

The calibration sections include the graduate G and the valve assembly V in channel assembly 1 and the glass bulb B in channel assembly 2. The Pyrex graduate G was calibrated with 0.05 ml divisions and encased in an evacuated Pyrex glass jacket. The vacuum jacket insulation prevented extraneous heat from entering the graduate and producing unwanted superfluid flow via the fountain effect.

Figure 3, channel assembly 1 demonstrates the construction of the stainless-steel valve assembly V. The valve was turned and polished at an angle of 45° and the valve seat edge was rounded and polished. The screw was turned by a control rod through the top of the Dewar system. An annular channel was formed by the valve rod and guide when the valve was a few turns open. However, the valve could be unscrewed sufficiently to eliminate the annular channel. The dimensions of this annular valve guide channel are listed in Table I.

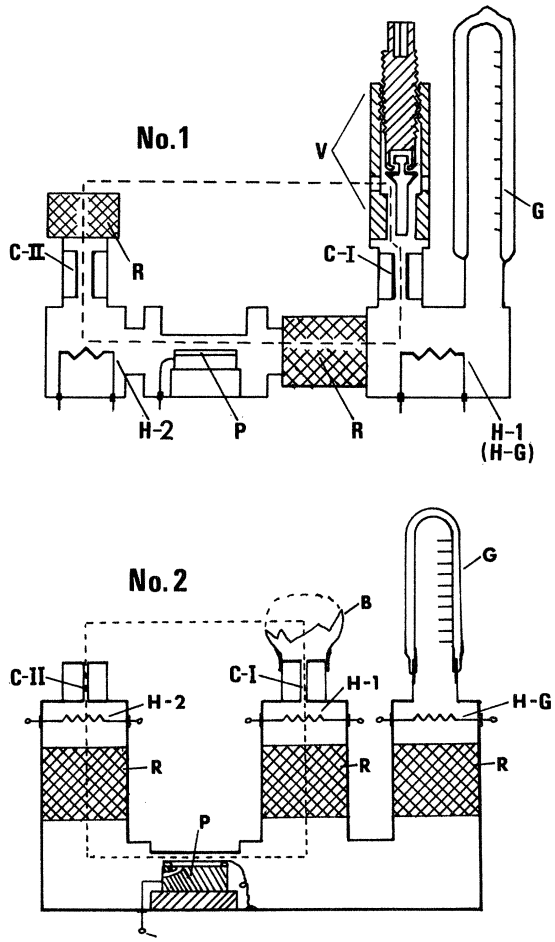

FIG. 3. Channel Assemblies No. 1 and No. 2. C-I and C-II are precision channels; the R's are packed jewelers-rouge porous plugs; P is the velocity probe; G is a vacuum-jacketed milliliter graduate with 0.05-ml divisions, and the dashed line represents the path of the circulation integral. In channel assembly No. 1, H-1 and H-2 are 605-Ω resistance heaters supported by stubakoffs and V is the valve assembly. In channel assembly No. 2, H-1, H-2, and H-3 are 211-Ω resistance heaters and B is a thin glass bulb with Kovar seal.

Glass bulb B as shown in channel assembly 2 sealed channel I. The control rod with a brass weight on the bottom was used to break the glass bulb when channel I was to be used. Cotton placed inside the bulb prevented glass from falling into the channel and was pushed aside by the control rod.

Calibration of the velocity probe was accomplished by measuring the volume flow rate of the superfluid through the velocity-probe channel and correlating it with the change in frequency. With the apparatus stabilized at a selected temperature and the helium-bath level midrange on the graduate,

superfluid was pumped into the graduate via the fountain effect by a constant voltage on heater H-G. When using channel assembly 1, valve V was closed, and when using channel assembly 2, the glass bulb B was unbroken, so the total fluid going into the graduate passed through the velocity-probe channel. The frequency change was displayed on the y axis of the recorder while the pen moved along the x axis linearly in time from a ramp voltage input. While the fluid level rose in the graduate, the recorder pen was lifted momentarily each time the level passed a 0.05 ml mark on the graduate. From this, the volume flow rate was calculated and the frequency change noted.

A calibration was made at 1.95 °K during each experimental session. It was found that the probe sensitivity changed when the temperature was cycled to room temperature and back. In a previous pressure-measuring experiment[16] the Bernoulli pressure was measured for superfluid flow over the temperature range 1.71–2.1 °K. Taking into account the appropriate superfluid density there was no discrepancy found. Therefore, it was not deemed necessary to calibrate at more than one temperature. However, a comparison check was made which showed a deviation of less than 8% at 2.1° and about 5% at 1.72°. The accuracy of the calibration curves for points near the critical velocity was estimated to be about 10%. It was possible to detect, under good conditions, a velocity of 0.05 cm/sec in the probe channel with a signal-to-noise ratio of approximately 2–1.

PROCEDURE

Essentially the same data-gathering procedure was used for both channel assemblies. While using channel assembly 1, valve V was open and when using channel assembly 2, bulb B was broken with the cotton pushed aside. With the channels immersed well below the liquid-helium level and the milliliter graduate full, superfluid was pumped via the thermomechanical effect by applying a voltage to heater H-1. Superfluid flowed toward H-1 in through channel I, as well as through channel II and the velocity-probe channel P. This arrangement constituted two parallel channels for superfluid flow with the relative proportion of flow through each channel being governed by the phase coupling. Because of the rouge plugs all of the normal fluid flowed into the bath through channel I. Therefore, pure superfluid or isothermal flow existed in channel II and channel P while a modified heat current was present in channel I. The cross sections A_1, A_2, and A_p of channels I, II, and P were much smaller than the connecting channels in the channel assemblies. Thus, with zero circulation around the dotted lines, Eq. (1) becomes

$$v_{s2}L_2 + v_{sp}L_p - v_{s1}L_1 = 0, \tag{3}$$

which gives the relation for the ratio of superfluid flow between the channels. The criteria in designing the assemblies and channel sizes were to insure that the velocity in channel II went critical first as the total superfluid flow was increased. Assuming the critical velocity is the effect of generating some form of vorticity as Feynman suggests, the characteristic size d and area of the channels were chosen with the following considerations. First, to insure that the superfluid flow did not go critical in channel P before channel II, the critical volume flow rate through channel P had to be greater than that through C-II:

$$\dot{V}_{spc} > \dot{V}_{s2c} . \tag{4}$$

Since the volume flow rates were equal, the velocities were related by

$$v_{sp} = (A_2/A_p)\, v_{s2} . \tag{5}$$

Substituting Eq. (5) into Eq. (3), a relation for the velocities of channels I and II was obtained:

$$v_{s2}[\, L_2 + (A_2/A_p)\, L_p] = v_{s1} L_1 . \tag{6}$$

To insure that the channel-II velocity went critical first, the apparatus was constructed so that

$$v_{s2c} < \frac{L_1}{L_2 + (A_2/A_p)\, L_p}\, v_{s1c} . \tag{7}$$

To make a critical-velocity measurement, the superfluid flow was gradually increased by heater H-1 voltage. The voltage was increased slowly by manually turning a 10-turn potentiometer to insure that superfluid acceleration effects were negligible. Figure 4 shows two examples of critical-velocity measurement runs. They are x-y recorder tracings of frequency-versus-heater H-1 voltage. To the left of point x on the curves the frequency change shows the gradual increase of superfluid flow through channel II. During this interval the phase coupling governed the relative amount of superfluid entering each channel, as described in Eq. (6) when zero circulation was present. At point x, the superfluid flow into channel II stopped increasing and remained constant to point y, while the superfluid flow in channel I increased more rapidly as the heater voltage was being gradually increased. Thus, the superfluid flow in channel II approached or reached its critical velocity at point x, while the impedance to superfluid flow remained zero in channel I. Beyond point y there was impedance to superfluid flow in channel I as evidenced by the rapid increase of flow in channel II. Therefore, the superfluid flow reached critical velocity in channel I at point y.

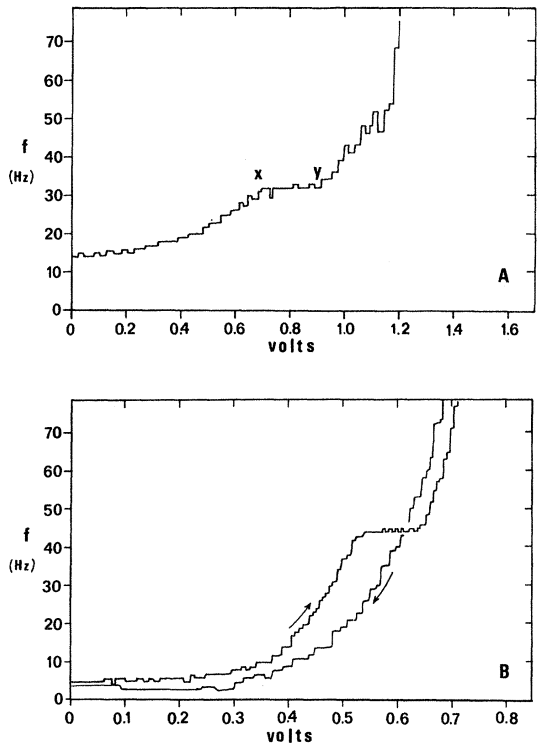

FIG. 4. Critical-velocity data curves. Two examples of x-y recorder tracings of frequency versus heater (H-1) voltage. The ordinate or y axis is the 2 least significant digits of the oscillator frequency which was nominally 16 MHz. x is the point where v_{s_2} went critical and y is the point where v_{s_1} went critical.

The critical velocity in channel II was calculated by measuring the frequency change at point x and determining the He-II volume flow rate $\dot{V}$ from the calibration curve. The critical superfluid volume flow rate for 1.95° was calculated by

$$\dot{V}_{s2c} = (\rho/\rho_s)\,\dot{V} . \tag{8}$$

Since the calibrations were made at 1.95°, it was necessary to find an equivalent superfluid volume flow rate for data at other temperatures. By equating the Bernoulli pressure at 1.95° to the Bernoulli pressure at temperature T, we have

$$\dot{V}_s(T) = \left(\frac{\rho}{\rho(T)}\right)^{1/2} \left(\frac{\rho}{\rho(1.95)}\right)^{1/2} \dot{V}(1.95) . \tag{9}$$

The critical velocities in channel II were then calculated by

$$v_{s2c} = \dot{V}_{s2c}(T)/A_2 . \tag{10}$$

At point y where the superfluid flow in channel I went critical, the velocity was calculated as follows. The magnitude of the mass-flow rate of superfluid in channel I and channel II was equal to the mass flow rate of the normal fluid in channel I:

$$\rho_s A_1 v_{s1} + \rho_s A_2 v_{s2} = \rho_n A_1 \bar{v}_{n1} . \tag{11}$$

$\bar{v}_{n1}$ is the average velocity of the normal fluid, and is related to the applied power by

$$\bar{v}_{n1} = (1/\rho STA_1)\, V^2/R_1 . \tag{12}$$

V is the voltage, R_1 is the heater (H-1) resistance, and S the specific entropy. Combining Eqs. (11) and (12), we have

$$v_{s1c} = (1/A_1)[\,(\rho_n/\rho_s)\, V^2/\rho STR_1 - A_2 v_{s2c}\,] . \tag{13}$$

The value of the line integral from Eq. (3) at the point the flow in channel II went critical was never zero. Except for runs in one session the value was always positive, indicating that proportionally more superfluid flowed in through channel II than the dimensional design called for. This meant the circulation in the superfluid system involving the line integral was not zero. Therefore, in practice, the phase-coupling picture of Eq. (3) was not so simple. As evidenced, for example, by Reppy,[17] Zimmerman,[18] and van Alphen,[13] persistent currents can be present in multiply connected regions. It is also speculated that vortices remain pinned to walls and persist for long periods. Thus, the line integral of $\vec{v}_s = (h/m)\nabla\phi$ must include the gradient of the phase of any circulation or vortices present along the path of integration. For example, if persistent circulation or vortices were trapped in the rouge plugs or around the resistors, those parts of the integral would each contribute $(h/m)n\pi$. Since $h/m \sim 10^{-3}$, n need only be 10^2 for this part of the integral to be as large as $v_s L$ through the channels.

Another unknown in the phase coupling picture was the effect of the heat current existing in channel I and in the path of the line integral. A small superfluid density gradient is present in heat currents due to the temperature gradient. Since, in the quantum-mechanical treatment of superfluids $|\psi|^2 = \rho_s$, some modification to the order parameter and to the phase must be made. Velocity fluctuations and currents in the bath, due to heat and vibration entering the Dewar, must have also contributed to the integral.

In any event, these unknown contributions did not detract from the fact that phase coupling was present and was utilized effectively to measure critical velocities.

At this point one might wonder whether persistent circulation was present flowing through the velocity-probe channel. The measured critical velocities would be in error if that had been the case because the assumed zero-flow frequency would not have been correct. Consider a case in which the velocity of the persistent circulation is

in the opposite direction of the superfluid being pumped by heater H-1. As the heater voltage is raised, the resultant velocity in the probe channel would decrease to a minimum where both the persistent circulation velocity and the velocity of the superfluid being pumped were equal in magnitude. With a further increase of heater voltage, the net velocity would begin to increase as the velocity of the pumped superfluid became larger than the oppositely directed persistent current velocity. Therefore, the frequency would decrease to a minimum before increasing as the heater voltage is raised. This effect was rarely observed, if at all, and usually the frequency change was only a few Hertz. Since there was no reason to suspect a preferred direction to the circulation, this indicated that the phase coupling was not strong enough to maintain large persistent currents through the velocity-probe channel. To insure further that no residual flow in the velocity probe was present with a velocity in the same direction as the velocity of the pumped fluid flow the following procedure was used.

Heaters H-1 and H-2 were pulsed in various order with approximately 5 V of about 0.3 sec duration. This produced large superfluid velocities and accelerations in the channels. The frequency fluctuation settled enough after about 30 sec to observe any change of frequency from the original value. There was seldom more than a few Hertz change, which indicated that there was little or no flow remaining in the probe channel. The evidence indicates that the phase coupling was not strong enough to maintain flow through the channels and into the bath. However, during the initial check-out of the apparatus, evidence of persistent circulation was observed. During this time the velocity probe was not sealed by epoxy in the probe holder. Therefore, small channels on the sides and bottom of the probe in parallel with the probe channel existed. This multiply connected region which did not directly involve the bath showed evidence of large persistent circulation. For this reason the probe was epoxied into the holder.

Many different shaped curves were obtained in the course of a session. Each was a product of the history of the superfluid and the heater pump used. Curve shapes similar to the return path, shown by the lower curve in Fig. 4(b) were the most commonly produced. In those, the phase coupling was not properly set to effect enough flow in channel II compared to channel I. The curves selected to calculate critical-velocity data were only those which showed characteristics of Fig. 4(a) and the upper tracing in Fig. 4(b). In each of these, the trial was started with undetectable flow in the velocity-probe channel, and evidently the proper phase coupling to maintain an effective ratio of superfluid flow in each channel. It was found that there was a high probability of producing these characteristic curves when the voltage pulsing technique as described above was used. The trial was begun anywhere from 2 to 15 min later; the length of time elapsed made no detectable difference, except the noise was usually less for the longer time.

An attempt was made to vary the length of the valve-guide channel in channel assembly A to affect the phase coupling. In most cases the characteristic curves were easier to produce with the channel at its maximum length, but no quantitative correlation was made concerning the line integral.

In approximately 20% of the data curves, the frequency decreased slightly (2–4 Hz) between point x and point y. It is believed that the phase coupling became altered slightly, switching some of the superfluid from channel II to channel I.

DISCUSSION AND RESULTS

In general, the frequency fluctuations were less while taking critical-velocity data than during the time of calibration. The observed noise was due to U-tube-type oscillations between the free helium surfaces in the milliliter graduate tube and the bath. In either case, at lower temperatures the system became more noisy. This was partially due to the increased superfluid density, making superfluid flow fluctuations more effective in producing pressure fluctuations. At lower temperatures, the characteristic curves were more difficult to obtain, and during some runs the critical-velocity point could not be easily delineated, due in part to the increased system noise. Therefore, it was mandatory to reduce external vibrations from the experimental apparatus and wait long periods for oscillations to die.

Figure 4(b) shows typically how the superfluid flow decreased from above the critical velocities. The displacement of the final frequency (when the flow had been decreased to zero) from the initial frequency represents temperature drift. Persistent circulation was ruled out by the voltage-pulsing technique outlined above. Frequency drifts which occurred in this manner, usually not more than 3 or 4 Hz, were noted and compensation was made.

The mean value of the critical velocities for the channels was calculated for each session at every temperature. The mean values for a particular channel varied to some extent from session to session, and not all the sessions had data at the same temperatures. For this reason, the following procedure was used to compile the data to inspect for temperature dependence. The more reliable and complete data at 1.95° was averaged for each channel by weighting the mean values with the number of runs per session, which is just the total average

of all the runs for the particular channel. The percent deviation of the mean values from this weighted average was determined, and this deviation was then used to adjust the critical velocity values at the other temperatures before their weighted average was calculated. It was felt that these adjustments would give a better picture for temperature comparison. Figure 5 shows these critical-velocity values as a function of temperature. On the average there is about a 10% decrease in critical-velocity values from high to low temperature. Considering the accuracy of the experiment which has an estimated 20% error at temperatures other than 1.95°, the 10% decrease in critical velocities is not too significant.

In contrast to this, Chase[2] found a greater than 45% decrease over the same temperature range for superfluid critical velocities in heat currents in wide channels. This percent corresponds roughly with the normal-fluid density change producing higher normal-fluid velocities at lower temperatures, which suggests a normal-fluid velocity influence.

Heat current flow was present only in channels A and C. However, it was a modified heat current since only a portion of the total superfluid counterflowed with the normal fluid. For these channels, the temperature dependence is definitely not as large as 45% over the temperature range investigated, and not much different than the isothermal flow temperature dependence. It is conjectured that the same mechanism producing the critical velocities in the isothermal flow produced the critical velocities in the modified heat currents. If there is a normal-fluid turbulence or superfluid–normal-fluid interaction, it was not present for the data presented here, except possibly in channel C at 1.72 °K. It is concluded that there is little superfluid critical-velocity temperature dependence in wide channels for the temperature range investigated.

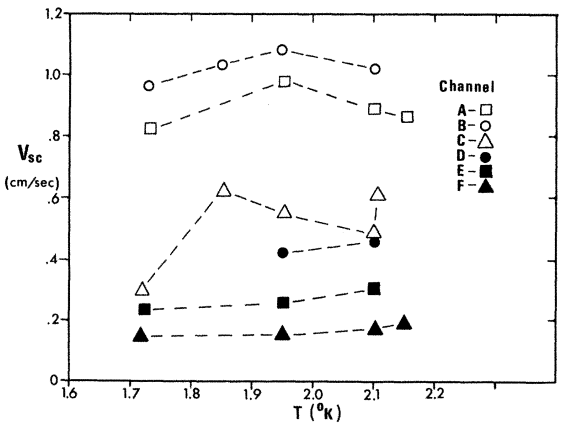

FIG. 5. Critical velocity versus temperature for all channels tabulated in Table I.

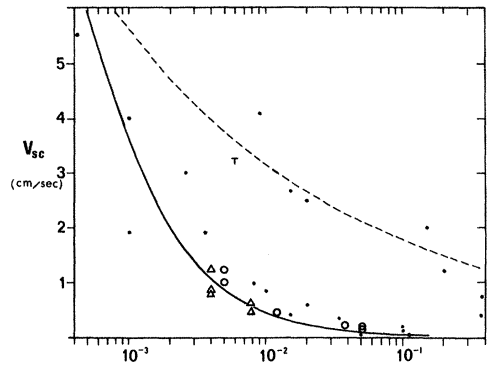

FIG. 6. Critical velocity versus channel dimension d: o is the isothermal flow; Δ is the heat current; T is the turbulent critical velocity; ● is the previously reported data from Refs. 1, 2, 7, 19; - - - $v_{sc}=d^{-1/4}$; 19, 1; ——— $v_{sc}=(2\hbar/md)\,[\ln 4d/a-\frac{7}{4}]$ (vortex ring model).

Figure 6 shows the mean critical-velocity data from each session at 1.95 °K as a function of d. The circles are for isothermal flow and the triangles are for the modified heat currents. The solid line is a plot of critical velocity versus d for vortex ring generation, with the vortex core equal to 10^{-8} cm. Theoretical calculations of critical velocities due to generation of line vortices are below the ring vortex curve.

The data, while displaced slightly above the ring vortex curve, is in good agreement with the Feynman vortex model for critical velocities. It can be seen that the critical velocity in channel E with the circular cross section is larger for its channel depth than the critical velocities in the rectangular channels. However, not enough is known about the mechanism for generating vortices or the configuration of the vortices produced, and more data is needed to reach any conclusions concerning the effect of channel geometry upon critical velocity.

During the check-out phase of the velocity probes and during the data sessions at superfluid velocities above 2 cm/sec sharp pressure changes were observed to occur. Figure 7 shows two examples of the pressure transitions that appeared in the flow well above the superfluid critical velocity. The following is an interpretation of the cause for the various features. The lower curve is a recorder trace of the frequency change versus the voltage applied to heater H-2 for channel assembly 2. At point A ($\Delta f = 135$ Hz), a pressure transition occurred and the superfluid flow became turbulent in the velocity-probe channel. The velocity at this point was calculated to be 3.2 cm/sec. After point B the

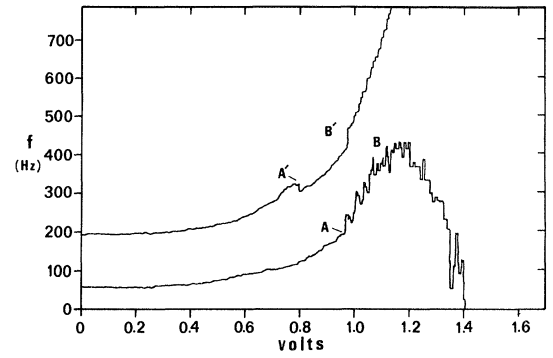

FIG. 7. Turbulent critical-velocity data curves. The ordinate is the 3 least significant digits of the oscillator frequency which was nominally 16 MHz. The upper curve is for flow through the velocity-probe channel with the static port on the upstream side of the superfluid flow. The lower curve is for flow in the opposite direction. Points A and A′ show flow transitions for the onset of superfluid turbulence. Beyond points B and B′ effects of the turbulent superfluid pressure gradient are the same order of magnitude as the Bernoulli pressure.

effect of the viscous pressure gradient, due to the turbulent superfluid flow, became as significant as the Bernoulli pressure, so that the magnitude of the total pressure on the foil decreased and then reversed. This was because the static-pressure port of the velocity probe was on the downstream side of the superfluid flow. In the upper curve where heater H-1 was used, the superfluid flow was in the other direction. In this case, the static pressure port was on the upstream side of the flow. At point A′, the pressure change occurred at the same velocity as at point A. Beyond A′ the pressure effect of the pressure gradient from the turbulent flow added to the Bernoulli pressure, causing the continually increasing curve. The jumps in the curve are probably the result of a flow switch with channel I.

The turbulent critical velocity of 3.2 cm/sec corresponds to the critical velocities reported by van Alphen *et al.*,[1] and is plotted by a T in Fig. 6 for comparison. A detailed study of these turbulent critical velocities was not performed, but many observations indicated flow transitions occurred in the 2- to 4-cm/sec velocity range. It is felt that van Alphen did not detect the small dissipation produced by generating vortices but rather observed the point where larger dissipation commenced with turbulent flow conditions.

It is concluded that superfluid phase coupling can be utilized effectively to control the superfluid flow in doubly connected regions in order to detect the velocity where flow impedance begins. A superfluid critical velocity exists for isothermal flow as well as heat currents in wide channels, which is the result of vortex generation as evidenced by its dependence upon channel depth. The critical velocity has at best only a weak dependence upon temperature in the range 1.71–2.15 °K. At velocities considerably higher than critical, flow transitions occur which are thought to be due to the onset of superfluid turbulence.

---

*Work supported by NASA Grant No. NGR 44-005-022 with assistance from Associated Western Universities AEC Grant No. AT(10-1) 1169 for summer support for one of us (A. F. H.) while at Los Alamos Scientific Laboratories, and faculty research support Grant from University of Houston.

†From a dissertation in partial fulfillment of the requirements for a Ph. D. degree. Present address: Galveston College, Galveston, Texas 77550.

[1]W. M. van Alphen, G. J. van Haasteren, R. de Bruyn Ouboter, and K. W. Taconis, Phys. Letters 20, 474 (1966).

[2]C. E. Chase, Phys. Rev. 127, 361 (1962); *Low Temperature Physics*, edited by R. O. Davies (Butterworths, London, 1963), Vol. 8, Chap. 3, p. 100.

[3]P. P. Craig and J. R. Pellam, Phys. Rev. 108, 1109 (1957).

[4]T. M. Wiarda and H. C. Kramers, in *Proceedings of the Eighth International Conference on Low Temperature Physics, London*, 1962, edited by R. O. Davies (Butterworths, London, 1963), pp. 98–99.

[5]R. J. Donnelly and O. Penrose, Phys. Rev. 103, 1137 (1956).

[6]R. J. Donnelly and A. C. H. Hallet, Ann. Phys. (N. Y.) 3, 320 (1958).

[7]W. J. Trela and W. M. Fairbank, Phys. Rev. Letters 19, 822 (1967).

[8]L. Onsager, Nuovo Cimento Suppl. 6, 249 (1949).

[9]R. P. Feynman. *Progress in Low Temperature Physics*, edited by C. J. Gorter (North-Holland, Amsterdam, 1955), Vol. I, p. 17.

[10]D. Y. Chung, in *Proceedings of the Eleventh International Conference on Low Temperature Physics, St. Andrew, Scotland*, 1968, edited by J. F. Allen, D. M. Finlayson, and D. M. McCall (University of St. Andrews Printing Department, St. Andrews, Scotland, 1969).

[11]J. F. Allen, D. J. Griffiths, and D. V. Osborne, Proc. Roy. Soc. (London) A287, 328 (1965).

[12]P. Sikora, E. F. Hammel, and W. E. Keller, Physica 32, 1693 (1966).

[13]W. M. van Alphen, R. de Bruyn Ouboter, K. W. Taconis, and E. van Sprosen, Physica 39, 109 (1968).

[14]E. Smith, R. Walton, H. V. Bohm, and J. D. Reppy, Phys. Rev. Letters 18, 637 (1967).

[15]A. F. Hildebrandt, H. Wahlquist, and D. D. Elleman, J. Appl. Phys. 33, 1798 (1962).

[16]H. E. Corke and A. F. Hildebrandt, Phys. Fluids II, 465 (1968).

[17]J. D. Reppy and D. Depatie, Phys. Rev. Letters

12, 187 (1964).
[18]J. B. Mehl and W. Zimmerman, Jr., Phys. Rev. Letters 14, 815 (1965).
[19]K. R. Atkins, *Liquid Helium* (Cambridge U. P., New York, 1959).

PHYSICAL REVIEW A VOLUME 2, NUMBER 4 OCTOBER 1970

Runaway Solutions: Remarks on the Asymptotic Theory of Radiation Damping*

William L. Burke†
Lick Observatory, Board of Studies in Astronomy and Astrophysics, University of California, Santa Cruz, California 95060
(Received 13 April 1970)

This paper examines the "runaway solutions" (exponentially diverging solutions) which often arise in slow-motion approximations such as classical electron theory. Detailed study of a typical runaway shows that it is a spurious solution attributable to faulty approximation technique rather than a physical result connected with, for example, the point-electron assumption. Methods for consistently using the slow-motion approximation while avoiding these spurious solutions are given.

In this paper we will discuss some general features that arise in systems where one has an oscillator coupled to a field (continuum) capable of transmitting waves with a finite speed. One expects the coupling both to lower the frequency of the oscillator due to an increased effective inertia and also to cause the amplitude of the oscillator to decay due to energy lost in outgoing radiation. For systems where the oscillator is much smaller than a wavelength of the resulting radiation, these effects are computable by perturbation theory. However, along with the physically reasonable solutions, one also finds unexpected solutions characterized by an exponential growth which is obviously physically impossible. These impossible solutions grow on a time scale so short that the initial mathematical assumptions of the perturbation scheme are violated. Hence, the occurrence of such solutions must be due to faulty perturbation technique. The problem is not a routine singular perturbation problem, but incorporates special features coming from delay terms implicit in the equations. The delay expresses the dependence of the motion on its past history and is due to the finite propagation speed of the medium to which the oscillator is coupled. Runaway solutions seem to be a common feature of systems incorporating a delay mechanism. Such spurious solutions have arisen in many places, most notably in classical electromagnetism,[1,2] where a great deal of effort has been expended in trying to interpret the results physically. Here we shall discuss this phenomenon in detail, using a simple mechanical system as a concrete example. For such a system, explanations involving infinite negative self-energies or noncausal behavior over short times are clearly inappropriate. Instead, we will resolve the difficulties by a careful use of ideas from singular perturbation theory.

The system that we will use as an example consists of a spherical elastic shell which oscillates radially, radiates acoustic waves, and suffers radiation damping.

Let $\tilde{r}$, $\tilde{t}$ equal the dimensional radius and time coordinates, l equal the equilibrium radius of the sphere, $Z(\tilde{t})$ equal the radial position of the sphere at time $\tilde{t}$, a_0 equal the speed of sound, and $\tilde{\phi}$ equal the velocity potential. If $\tilde{\phi}$ satisfies

$$\nabla_{\tilde{r}}^2 \tilde{\phi} - \frac{1}{a_0^2} \frac{\partial^2 \tilde{\phi}}{\partial \tilde{t}^2} = 0, \tag{1}$$

then we can arrive at a solution of the linearized fluid equations by taking a velocity given by

$$\vec{v} = \vec{\nabla} \tilde{\phi} \tag{2}$$

and a pressure given by

$$p - p_0 = \rho_0 \frac{\partial \tilde{\phi}}{\partial t}, \tag{3}$$

where p_0 and ρ_0 are the static pressure and density of the medium. The boundary conditions are the expression

$$\frac{\partial \tilde{\phi}}{\partial \tilde{r}} [Z(t)] = \frac{dZ}{d\tilde{t}} \tag{4}$$

and the restriction to outgoing waves for large $\tilde{r}$.

We can introduce the mechanical parameters of the elastic shell by means of an "effective mass" m and "effective elasticity" k such that the equation of motion for the shell becomes